Cumhuriyet Sci. J., 44(3) (2023) 504-509
DOI: https://doi.org/10.17776/csj.1284327

Cumhuriyet Science Journal

| csj.cumhuriyet.edu.tr | Founded: 2002 ISSN: 2587-2680 e-ISSN: 2587-246X Publisher: Sivas Cumhuriyet University

Effect of Synthesizing Process on the Formation of Fe_3O_4 Magnetic Nanoparticles

Cemal Aka [1,a], Mustafa Akyol [1,b,*]

[1] *Department of Materials Science and Engineering, Adana Alparslan Türkeş Science and Technology University, 01250 Adana, Türkiye*
**Corresponding author*

Research Article

History
Received: 17/04/2023
Accepted: 28/08/2023

ABSTRACT

In this work, the effect of synthesizing process on the morphology, structure, and magnetic properties of Fe_3O_4 magnetic nanoparticles have been studied by performing X-ray diffraction, scanning electronic microscopy, and vibrating sample magnetometer measurements. Fe_3O_4 nanoparticles were synthesized by hydrothermal and solvothermal methods. X-ray diffraction analysis revealed that both samples have cubic crystal phase. However, Fe_2O_3 impurity peaks were observed in the sample synthesized by hydrothermal method. The crystallite sizes of samples synthesized by hydrothermal and solvothermal methods were approximately 38 and 24 nm, respectively. The scanning electron microscope images show that spherical porous and cubic shape Fe_3O_4 nanoparticles were obtained by solvothermal and hydrothermal method, respectively. The average particle sizes of Fe_3O_4 samples synthesized by hydrothermal and solvothermal methods were determined as 220 and 450 nm, respectively. Both samples behave a soft ferromagnetic characteristic having almost zero coercive field. The magnetic saturation values of Fe_3O_4 nanoparticles synthesized by hydrothermal and solvothermal methods were determined as 28.78 and 77.31 emu/g, respectively. As a result of the characterizations, porous Fe_3O_4 nanoparticles synthesized by solvothermal method show better crystal structure, morphological and magnetic properties than Fe_3O_4 nanoparticles synthesized by hydrothermal method.

Keywords: Fe_3O_4, Magnetic nanoparticles, Hydrothermal, Solvothermal, Magnetic hysteresis.

[a] *cemalakaa@gmail.com* *https://orcid.org/0009-0009-3780-0822* [b] *makyol@atu.edu.tr* *https://orcid.org/0000-0001-8584-0620*

Introduction

Magnetic materials have an important place in modern technology. One of the most commonly used magnetic material is magnetite (Fe_3O_4) due to its low cost, low toxicity and good magnetic properties [1]. It is a ferrimagnetic material because its crystal lattice is composed of FeO and Fe_2O_3 that means its Fe (II) and Fe (III) ions are unequal in magnitude and aligned in antiparallel direction. In addition, Fe_3O_4 exhibits better conductivity at room temperature than some other metal oxides in the same category [2-4]. Generally, physical and chemical properties of magnetic nanomaterials depend on their morphology and size [5]. As a result of the tuning physical and chemical properties, many usage areas of Fe_3O_4 nanoparticles have emerged in technology. Fe_3O_4 nanoparticles can be used as catalysts [6], drug delivery systems [7], magnetic resonance imaging [8], antibacterial agents [9], heavy metal absorbers [10], and for solar thermal energy harvesting [11]. In addition, nanocomposite materials including Fe_3O_4 nanoparticles can be used as electrochemical sensors and radar absorbing materials [12-14]. Various synthesis methods have been developed to increase the magnetic properties and application areas of Fe_3O_4 nanoparticles. Some of synthesis methods of Fe_3O_4 nanoparticles can be listed as hydrothermal [15], co-precipitation [16], thermal decomposition [17] and sol-gel [18]. Co-precipitation method is a simple, inexpensive and easy way to synthesize Fe_3O_4 [19]. In the co-precipitation method, Fe_3O_4 can be obtained by precipitating Fe (II) and Fe (III) ions in an alkaline medium (1:2 ratio). As a result of the reaction, single and multicomponent Fe_3O_4 particles can be synthesized [20]. Thermal decomposition method is known as one of the best ways to synthesize nanomaterials with controllable size and morphology. However, the compounds used in the synthesis are toxic and additionally require relatively high temperatures [21, 22]. Hydrothermal and solvothermal methods are almost identical, but there is a fundamental difference. Hydrothermal synthesis is synthesis through chemical reactions in an aqueous solution above the boiling point of water. On the other hand, solvothermal synthesis is a synthesis that takes place in a non-aqueous solution at relatively high temperatures. Hydrothermal/solvothermal synthesis methods have more advantageous than other listed methods above. Although these methods are generally considered low-efficiency, this problem can be solved by adjusting the critical temperature and pressure value of almost all materials and solvent systems [23]. Nanomaterials can be synthesized under high vapor pressure with minimum material loss. Thus, high quality nanostructured materials can be synthesized by hydrothermal and/or solvothermal methods [23]. *Radoń et al.* investigated the structure and optical properties of Fe_3O_4 nanoparticles synthesized by co-precipitation with different organic modifiers [24]. They synthesized Fe_3O_4

nanoparticles with different crystal size in the range of 2.9-12.2 nm and band gap ranging from 2.6-3.01 eV by co-precipitation method. *Ahmadi et al.* synthesized Fe_3O_4 nanocrystals using the hydrothermal approach and studied some of their structural and physical properties [25]. They found that crystallite size, particle size and saturation magnetization increase with reaction temperature. *Lemine et al.* synthesized Fe_3O_4 nanoparticles by sol-gel method and studied their magnetic properties [26]. The synthesized Fe_3O_4 nanoparticles have a particle size of 8 nm. Since it is the lower than the critical size for superparamagnetic property, the Fe_3O_4 nanoparticles have a for hyperthermia applications.

In this study, Fe_3O_4 nanoparticles were synthesized by hydrothermal and solvothermal methods. The differences between these two very similar methods are revealed by examining their crystal structure, morphology, and magnetic properties. The results showed that the solvothermal method has better crystal structure, morphology, and magnetic properties than the hydrothermal method.

Experimental Procedure

Materials

Iron (III) chloride hexahydrate-$FeCl_3{\cdot}6H_2O$ (Sigma-Aldrich), Iron (II) chloride tetrahydrate-$FeCl_2{\cdot}4H_2O$ (Sigma-Aldrich), Sodium hydroxide-NaOH (Sigma-Aldrich) were used to hydrothermal synthesis method. Iron (III) chloride hexahydrate-$FeCl_3{\cdot}6H_2O$ (Sigma-Aldrich), Polyvinylpyrrolidone (PVP)- $(C_6H_9NO)_n$ (BioShop), Sodium acetate- NaAc, Ethylene glycol-$C_2H_6O_2$ (ISOLAB chemicals) were used to solvothermal synthesis method.

Synthesis of Fe_3O_4

Hydrothermal synthesis

The hydrothermal method was used to synthesize Fe_3O_4 nanoparticles. Figure 1 shows the schematically illustrated synthesizing procedure (blue arrows) of Fe_3O_4 nanoparticles. $FeCl_2{\cdot}4H_2O$ (0.288 g) and $FeCl_3{\cdot}6H_2O$ (0.799 g) were dissolved in 50 ml distilled water. Then, 0.8 g NaOH was dissolved in 10 ml of distilled water to obtain a 2M NaOH solution. 2M NaOH solution was slowly added dropwise to mixture [25]. The mixture was transferred into a 100 ml Teflon and then into the Teflon-lined stainless-steel autoclave and sealed for heating at 200 ºC for 8 h. As a result of the reaction, Fe_3O_4 nanoparticles were obtained and washed with ethanol several times. Finally, it was dried at 75 ºC for 24 h and brown color Fe_3O_4 nanoparticles were obtained. This sample is called as #1-Fe_3O_4.

Solvothermal synthesis

Here, the Fe_3O_4 nanoparticles were synthesized by the following procedure as green color arrows shown in Fig.1. $FeCl_36H_2O$ (1.5 g), PVP (1.0 g), and NaAc (2.0 g) were added into 30 mL of ethylene glycol [15]. To make sure all the ingredients completely dissolved, the liquid was rapidly mixed for 2 hours. Then, the mixture was transferred to a 100 ml Teflon-lined stainless-steel autoclave and sealed for heating at 200 ºC for 8 h. As a result of the reaction, Fe_3O_4 nanoparticles were obtained and washed with ethanol several times. Finally, it was dried at 75 ºC for 24 h and black color Fe_3O_4 nanoparticles were obtained. This sample is called as #2-Fe_3O_4.

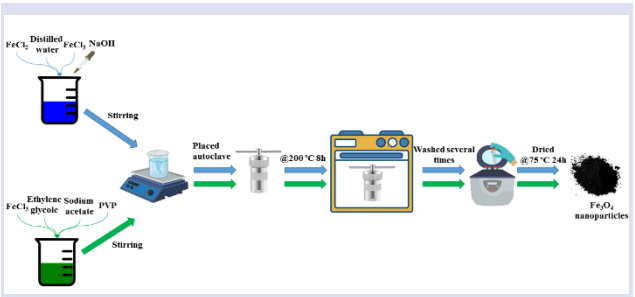

Figure 1. Schematically illustrated synthesizing process of Fe_3O_4 magnetic nanoparticles.

Characterization Techniques

X-ray diffractometer (XRD) with Cu-Kα radiation was used to analyze some structural properties of particles. Morphology and surface properties of samples were examined by scanning electron microscope (SEM). Vibrating sample magnetometer (VSM) was used to characterize the magnetic properties of magnetic particles at room temperature.

Results and Discussions

Structural Analysis

The structural properties of Fe_3O_4 nanoparticles synthesized by different methods were investigated by XRD. Figure 2 indicates the XRD patterns of Fe_3O_4 nanoparticles synthesized by different methods. The diffraction peaks in both samples are at 2ϑ = 18.38, 21.61 30.24, 35.58, 37.12, 42.96, 53.49, 56.92, 62.68, 71.28 and 74.05 angles which are corresponding to (111), (002), (311), (222), (400), (422), (511), (440), (620) and (553) planes, respectively. These peaks indicate the formation of cubic Fe_3O_4 crystals. In the hydrothermal method, in addition to main crystal peaks, two impurity peaks belonging to Fe_2O_3 phases which are indicated by * symbol, have been observed in sample #1-Fe_3O_4. These impurity peaks might be occurred due to insufficient reaction time. The lattice parameters of #1-Fe_3O_4 and #2-Fe_3O_4 samples are found as 8.376 Å and 8.395 Å, respectively. The crystallite sizes of the samples were calculated by using the basic Scherrer equation [27].

$$D = \frac{K\lambda}{\beta\, cos\theta} \quad (1)$$

where D is the crystallite size, λ is the x-ray wavelength (CuKα = 1.5406 Å), β is the width of the x-ray peak on the 2ϑ axis measured as full width at half

maximum (FWHM), ϑ is the Bragg angle, K is the so-called Scherrer constant. K depends on the crystallite shape and the size distribution, indices of the diffraction line, and the actual definition used for β whether FWHM or integral breadth [28]. K can have values anywhere from 0.62 and 2.08. In this paper, K = 0.9 was used. The calculated average crystallite sizes of #1-Fe_3O_4 and #2-Fe_3O_4 samples are found as 38 nm and 24 nm, respectively.

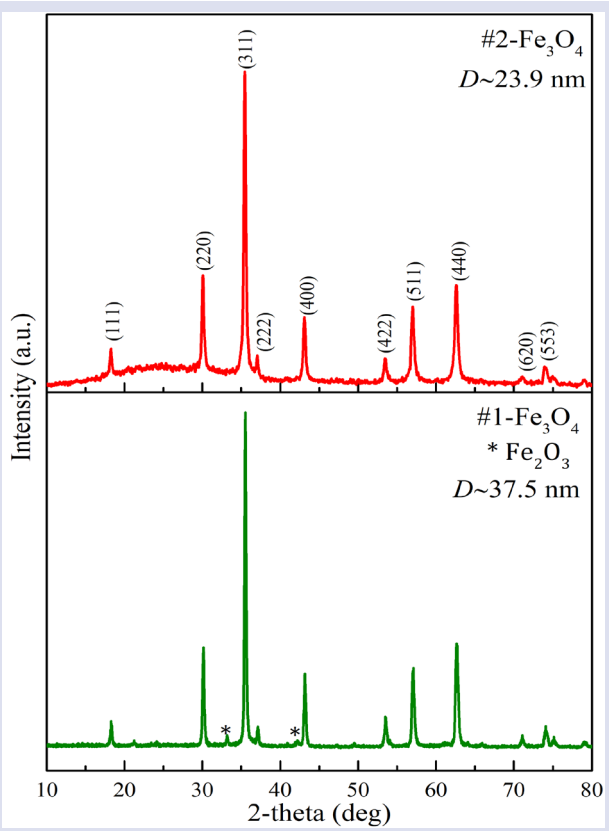

Figure 2. X-ray diffraction patterns of #1-Fe_3O_4 and #2-Fe_3O_4 samples.

Morphological Analysis

The morphologies of the synthesized samples were analyzed by using the SEM imaging technique. SEM images taken at various magnitudes and particle size distribution histogram of Fe_3O_4 nanoparticles produced by hydrothermal method are given in Figs.3a-d. In Figs. 3a-c, it is seen that Fe_3O_4 nanoparticles were successfully synthesized by hydrothermal method. The particles are formed as cubic shape and they are almost uniformly and homogenously distributed through the sample. The particle size distribution histogram of #1-Fe_3O_4 sample is given in Fig. 3d. The histogram was created by randomly selected 100 particles in the SEM images. The sizes of Fe_3O_4 nanoparticles are between 100 and 500 nm. The average particle size was found as 220 nm by taking lognormal fitting of experimental data as shown a red color curve in Fig.3d.

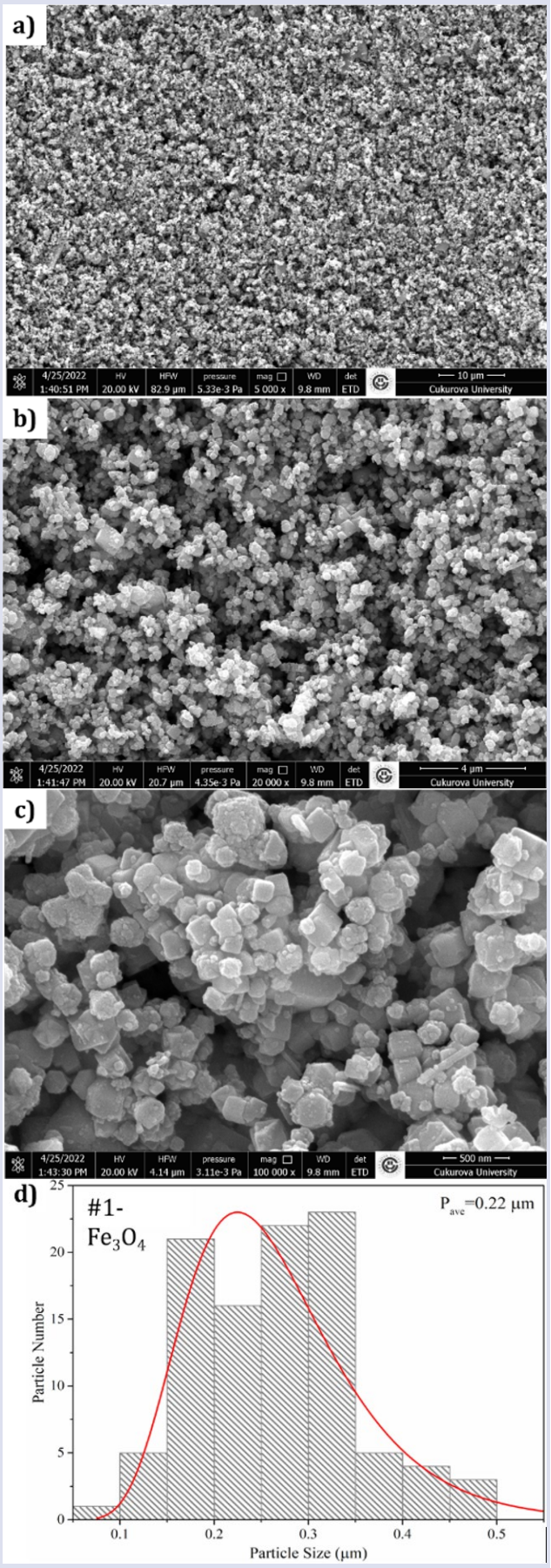

Figure 3. a-c) SEM images and d) particle size distribution histogram of #1-Fe_3O_4 sample.

The images in Fig.3 show that the nanocrystals synthesized by hydrothermal method form finite aggregate crystals due to its high surface energy. The particle size difference may be due to the variation of the dropping rate of NaOH. Because of fast dropping of NaOH solution, the Fe_3O_4 crystals form agglomerate and stick together having different sizes.

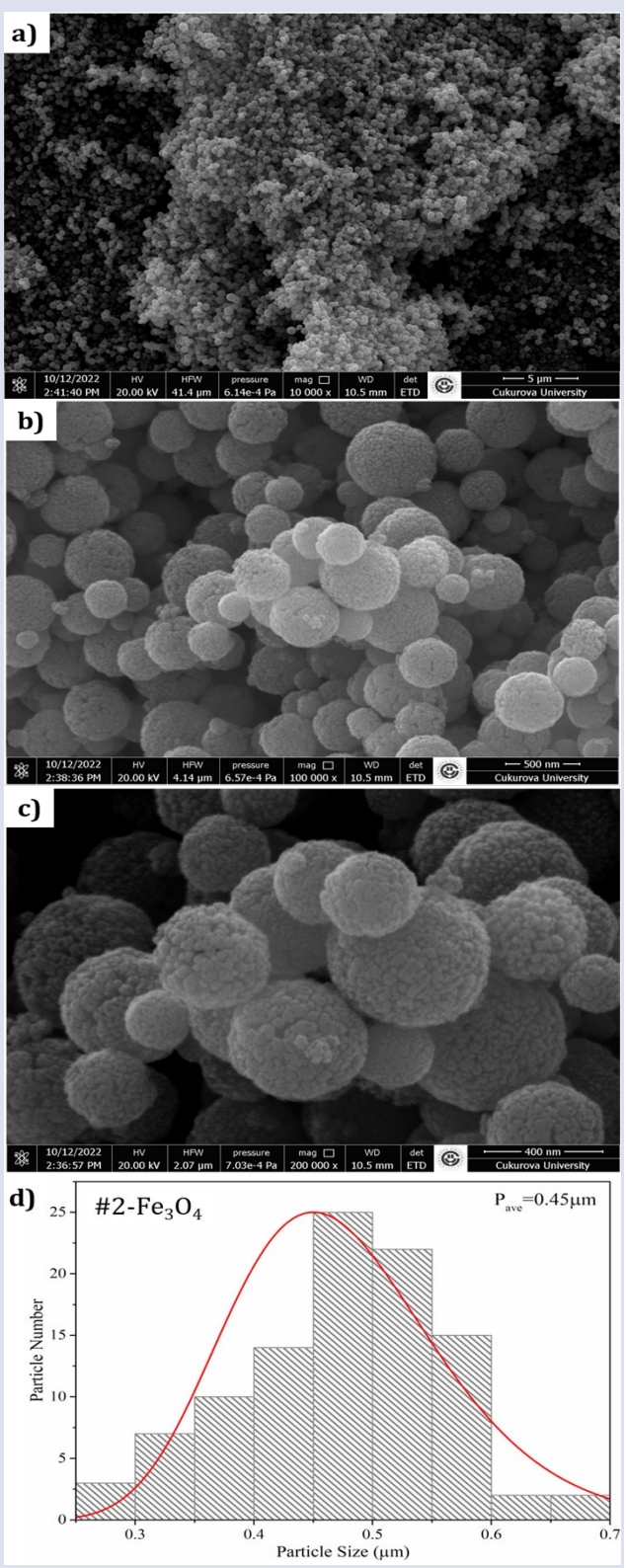

Figure 4.a-c) SEM images and d) particle size distribution histogram of #2-Fe_3O_4 sample.

SEM images taken at various magnitudes and particle size distribution histogram of #2-Fe_3O_4 sample produced by solvothermal method are given in Figs.4a-d. In Figs. 4a-c, in contrast to #1-Fe_3O_4 sample, spherical and porous shape Fe_3O_4 nanoparticles were successfully synthesized by solvothermal method. Similarly, the particle size distribution histogram of porous Fe_3O_4 nanoparticles were created by randomly selected 100 grains in the sample (see Fig.4d). The particle sizes of #2-Fe_3O_4 sample are between 200 and 700 nm. The average particle size was found as 450 nm by taking lognormal fitting of experimental data as shown a red color curve in Fig.4d. When the average particle size is compared between two samples, it is clearly seen that the #2-Fe_3O_4 sample's size is almost $\times 2$ larger than #1-Fe_3O_4 sample. The increment in the particle size might be related to the lower atmosphere pressure in the solvothermal method than the hydrothermal method. *Zhu et al.* studied the reaction conditions such as precursor, capping agent, precipitation agent concentration, reaction temperature and reaction time to understand the formation mechanism of porous Fe_3O_4 nanospheres [15]. The regularity of morphology and particle size can be adjusted by changing the amount of $FeCl_3$, reaction temperature and time, amount of NaAc and amount of PVP [15].

Magnetic Analysis

Magnetic hysteresis (*M(H)*) measurements of the synthesized Fe_3O_4 nanoparticles were performed at room temperature under ∓ 2T magnetic field range. *M(H)* curves of #1-Fe_3O_4 and #2-Fe_3O_4 coded nanoparticles are given in Fig.5. It is understood from the hysteresis curves that the samples have no coercive field values and behaves like a ferrimagnetic characteristic. It can be said that the XRD and *M(H)* curves are consistent with each other, since both samples were found as inverse spinel structure. The saturation magnetization values were determined as 28.78 emu/g and 77.31 emu/g for the #1-Fe_3O_4 and #2-Fe_3O_4 coded samples, respectively. The increase in magnetization with the increase of particle size in the #2-Fe_3O_4 rather than #1-Fe_3O_4 sample is expected. In addition to size effect, since the magnetization of the Fe_2O_3 crystal which is observed in #1-Fe_3O_4 sample, is very small compared to Fe_3O_4, it is thought to reduce the total magnetization [29].

Further, we calculate the effective magnetic moment from the following equation,

$$\mu_{eff} = \frac{MM_S}{N_A\beta} \qquad (2)$$

where M is the molecular weight, N_A is the Avogadro's number and β is the conversion factor (9.27×10^{-21} erg/Oe). The effective magnetic moment values are found as 1.19 μ_B and 3.21 μ_B for #1-Fe_3O_4 and #2-Fe_3O_4 coded samples, respectively. Since there is

a linear relation between particle size and moment, the reason of higher moment value of #2-Fe_3O_4 sample is related to the relatively its large particle size. But it is still lower than the theoretical value (4 μB)[30, 31]. The calculated effective magnetic moments of Fe_3O_4 magnetic nanoparticles are consistent with the previously reported studies[30-32].

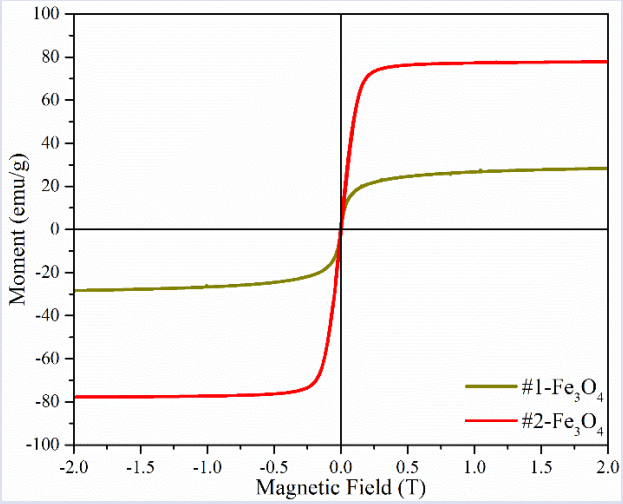

Figure 5. Magnetic hysteresis curves of #1-Fe_3O_4 and #2-Fe_3O_4 samples.

Table 1. Structural and magnetic parameters of #1-Fe_3O_4 and #2-Fe_3O_4 magnetic nanoparticles.

Sample Code	*D* (nm)	*P* (nm)	M_s (emu/g)	μ_{eff} (μ_B)
#1-Fe_3O_4	38	220	28.78	1.19
#2-Fe_3O_4	24	450	77.31	3.21

Conclusions

In summary, the effect of hydro-/solvothermal methods on the structure, morphology, and magnetic properties of Fe_3O_4 magnetic nanoparticles were studied in this work. It is found that the synthesizing procedure affects the morphology of the Fe_3O_4 particles that cubic and porous spherical shape Fe_3O_4 nanoparticles were determined when they are synthesized by hydrothermal and solvothermal methods, respectively. In addition, although both samples have similar magnetic characteristic, #2-Fe_3O_4 sample has almost ×2.5 higher magnetic saturation than #1-Fe_3O_4 sample. The difference in saturation magnetization might come from the particle size effect and/or Fe_2O_3 impurity phases which is observed in #1-Fe_3O_4 sample. It was determined that the solvothermal method showed much better crystal structure, morphology, and magnetic properties than the hydrothermal method.

Conflicts of interest

The authors stated that did not have conflict of interests.

Acknowledgement

This work is supported by the Adana Alparslan Türkeş Science and Technology University Scientific Research Council under Project Number: 22303006.

References

[1] Zhao T., Hierarchical Bi2O2CO3 microspheres with improved visible-light-driven photocatalytic activity, *Cryst. Eng. Comm.*, 13 (2011) 4010-4017.

[2] Miles P.A., Westphal W.B.,A. Von Hippel, Dielectric Spectroscopy of Ferromagnetic Semiconductors, *Reviews of Modern Physics*, 29 (1957) 279-307.

[3] Evans B.J., Experimental studies of the electrical conductivity and phase transition in Fe3O4. *AIP Conference Proceedings*, 24 (1975) 73-78.

[4] Vella L. D. Emerson, Electrical Properties of Magnetite- and Hematite-Rich Rocks and Ores, *ASEG Extended Abstracts*, 2012 (2012) 1-4.

[5] Qiao L., Standardizing Size- and Shape-Controlled Synthesis of Monodisperse Magnetite (Fe3O4) Nanocrystals by Identifying and Exploiting Effects of Organic Impurities, *ACS Nano*, 11 (2017) 6370-6381.

[6] Arefi M., Superparamagnetic Fe(OH)3@Fe3O4 Nanoparticles: An Efficient and Recoverable Catalyst for Tandem Oxidative Amidation of Alcohols with Amine Hydrochloride Salts, *ACS Combinatorial Science*, 17 (2015) 341-347.

[7] Li Q., Xuan Y., Wang J., Experimental investigations on transport properties of magnetic fluids, *Experimental Thermal and Fluid Science*, 30 (2005) 109-116.

[8] Jordan A., Endocytosis of dextran and silan-coated magnetite nanoparticles and the effect of intracellular hyperthermia on human mammary carcinoma cells in vitro, *Journal of Magnetism and Magnetic Materials*, 194 (1999) 185-196.

[9] Prabhu Y.T., Synthesis of Fe3O4 nanoparticles and its antibacterial application, *International Nano Letters*, 5 (2015) 85-92.

[10] Kalantari K., Rapid Adsorption of Heavy Metals by Fe3O4/Talc Nanocomposite and Optimization Study Using Response Surface Methodology, *International Journal of Molecular Sciences*, 15 (2014) 12913-12927.

[11] Chen Y., Stably dispersed high-temperature Fe3O4/silicone-oil nanofluids for direct solar thermal energy harvesting, *Journal of Materials Chemistry A*, 4 (2016) 17503-17511.

[12] Narang S. S. Bahel, Low loss dielectric ceramics for microwave applications: A review, *Journal of Ceramic Processing Research*, 11 (2010) 316-321.

[13] Sanaeifar N., A novel electrochemical biosensor based on Fe3O4 nanoparticles-polyvinyl alcohol composite for sensitive detection of glucose, *Analytical Biochemistry*, 519 (2017) 19-26.

[14] Jian X., Facile Synthesis of Fe3O4/GCs Composites and Their Enhanced Microwave Absorption Properties, *ACS Applied Materials & Interfaces*, 8 (2016) 6101-6109.

[15] Zhu M. G. Diao, Synthesis of Porous Fe3O4 Nanospheres and Its Application for the Catalytic Degradation of Xylenol Orange, *The Journal of Physical Chemistry C*, 115 (2011) 18923-18934.

[16] Hariani P., Synthesis and Properties of Fe3O4 Nanoparticles by Co-precipitation Method to Removal

Procion Dye, *International Journal of Environmental Science and Development*, 4 (2013) 336-340.

[17] Kimata M., Nakagawa D., Hasegawa M., Preparation of monodisperse magnetic particles by hydrolysis of iron alkoxide, *Powder Technology*, 132 (2003) 112-118.

[18] Albornoz C., Jacobo S.E., Preparation of a biocompatible magnetic film from an aqueous ferrofluid, *Journal of Magnetism and Magnetic Materials*, 305 (2006) 12-15.

[19] Wang X., Fabrication and characterization of magnetic Fe3O4–CNT composites, *Journal of Physics and Chemistry of Solids*, 71 (2010) 673-676.

[20] Kentish S.E., Stevens G.W., Innovations in separations technology for the recycling and re-use of liquid waste streams, *Chemical Engineering Journal*, 84 (2001) 149-159.

[21] Rockenberger, J., Scher E.C., Alivisatos A.P., A New Nonhydrolytic Single-Precursor Approach to Surfactant-Capped Nanocrystals of Transition Metal Oxides, *Journal of the American Chemical Society*, 121 (1999) 11595-11596.

[22] Deng Y., Magnetic nanoparticles prepared in natural deep eutectic solvent for enzyme immobilisation, *Biocatalysis and Biotransformation*, 40 (2022) 450-460.

[23] Wang S., Recyclable solar evaporator based on hollow glass microspheres for water purification and desalination, *Journal of Environmental Chemical Engineering*, 10 (2022) 108254.

[24] Radoń A., Structure and optical properties of Fe3O4 nanoparticles synthesized by co-precipitation method with different organic modifiers, *Materials Characterization*, 131 (2017) 148-156.

[25] Ahmadi S., Synthesis of Fe3O4 nanocrystals using hydrothermal approach, *Journal of Magnetism and Magnetic Materials*, 324 (2012) 4147-4150.

[26] Lemine O.M., Sol–gel synthesis of 8nm magnetite (Fe3O4) nanoparticles and their magnetic properties, *Superlattices and Microstructures*, 52 (2012) 793-799.

[27] Scherrer P., Bestimmung der inneren Struktur und der Größe von Kolloidteilchen mittels Röntgenstrahlen, in *Kolloidchemie Ein Lehrbuch*, R. Zsigmondy, Editor., Springer Berlin Heidelberg: Berlin, Heidelberg. (1912) 387-409.

[28] Langford J.I., Wilson A.J.C., Scherrer after sixty years: A survey and some new results in the determination of crystallite size, *Journal of Applied Crystallography*, 11 (1978) 102-113.

[29] Bahari A., Characteristics of Fe3O4, α -Fe2O3, and γ-Fe2O3 Nanoparticles as Suitable Candidates in the Field of Nanomedicine, *Journal of Superconductivity and Novel Magnetism*, 30 (2017) 2165-2174.

[30] Li Q., Correlation between particle size/domain structure and magnetic properties of highly crystalline Fe3O4 nanoparticles, *Scientific Reports*, 7 (2017) 9894.

[31] Hedayatnasab Z., Abnisa F., Daud W.M.A.W., Review on magnetic nanoparticles for magnetic nanofluid hyperthermia application, *Materials & Design*, 123 (2017) 174-196.

[32] Rajan A., Sharma M., Sahu N.K., Assessing magnetic and inductive thermal properties of various surfactants functionalised Fe3O4 nanoparticles for hyperthermia, *Scientific Reports*, 10 (2020) 15045.